



HAL
open science

The role of attractive and repellent scene memories in ant homing (*Myrmecia croslandi*)

Trevor Murray, Zoltan Kocsi, Hansjürgen Dahmen, Ajay Narendra, Florent Le Moël, Antoine Wystrach, Jochen Zeil

► To cite this version:

Trevor Murray, Zoltan Kocsi, Hansjürgen Dahmen, Ajay Narendra, Florent Le Moël, et al.. The role of attractive and repellent scene memories in ant homing (*Myrmecia croslandi*). *Journal of Experimental Biology*, 2020, 223 (3), pp.jeb210021. 10.1242/jeb.210021 . hal-02886343

HAL Id: hal-02886343

<https://hal.science/hal-02886343v1>

Submitted on 16 Sep 2020

HAL is a multi-disciplinary open access archive for the deposit and dissemination of scientific research documents, whether they are published or not. The documents may come from teaching and research institutions in France or abroad, or from public or private research centers.

L'archive ouverte pluridisciplinaire **HAL**, est destinée au dépôt et à la diffusion de documents scientifiques de niveau recherche, publiés ou non, émanant des établissements d'enseignement et de recherche français ou étrangers, des laboratoires publics ou privés.

The role of attractive and repellent scene memories in ant homing (*Myrmecia croslandi*)

Trevor Murray¹, Zoltan Kocsi¹, Hansjürgen Dahmen², Ajay Narendra³, Florent Le Möel⁴,
Antoine Wystrach^{4†}, Jochen Zeil^{1†}

¹Research School of Biology, Australian National University, Canberra, Australia;

²Cognitive Neuroscience, University of Tübingen, Tübingen, Germany

³Department of Biological Sciences, Macquarie University, Sydney, NSW 2109, Australia

⁴Research Center on Animal Cognition, University Paul Sabatier/CNRS, Toulouse, France

† Co-last authors

Corresponding author: Trevor Murray, trevor.murray@anu.edu.au

Running title: Views and navigational information

Key words: Visual navigation, ants, attractive and repellent memories, homing, route following, *Myrmecia croslandi*

19 Abstract

20 Solitary foraging ants rely on vision when travelling along routes and when pinpointing their
21 nest. We tethered foragers of *Myrmecia croslandi* on a trackball and recorded their intended
22 movements when the trackball was located on their normal foraging corridor (on-route),
23 above their nest and at a location several meters away where they have never been before
24 (off-route). We find that at on- and off-route locations, most ants walk in the nest or foraging
25 direction and continue to do so for tens of metres in a straight line. In contrast, above the
26 nest, ants walk in random directions and change walking direction frequently. In addition, the
27 walking direction of ants above the nest oscillates at a fine scale, reflecting search movements
28 that are absent from the paths of ants at the other locations. An agent-based simulation
29 shows that the behaviour of ants at all three locations can be explained by the integration of
30 attractive and repellent views directed towards or away from the nest, respectively. Ants are
31 likely to acquire such views via systematic scanning movements during their learning walks.
32 The model predicts that ants placed in a completely unfamiliar environment should behave
33 as if at the nest, which our subsequent experiments confirmed. We conclude first, that the
34 ants' behaviour at release sites is exclusively driven by what they currently see and not by
35 information on expected outcomes of their behaviour. Second, that navigating ants might
36 continuously integrate attractive and repellent visual memories. We discuss the benefits of
37 such a procedure.

38 250 words

39

40 Introduction

41 Navigation on a local, in contrast to a global, scale involves travelling along routes and
42 pinpointing places (e.g. Zeil 2012). Much evidence has accumulated to show that ants form
43 visual memories of how the scene looks along routes (e.g. Wehner et al., 1996; Wystrach et
44 al., 2011; Mangan and Webb, 2012) and that alignment matching (Zeil et al., 2003; Collett et
45 al., 2013) between memorized and currently experienced views provides robust information
46 on heading direction (Graham and Cheng, 2009; Baddeley et al., 2011, 2012; Narendra et al.,
47 2013; Zeil et al., 2014). Heading direction can be recovered, even from locations at some
48 distance from familiar locations, by detecting the minimum of the rotational image difference
49 function resulting from a comparison between current and memorised views (rotIDF, Zeil et
50 al., 2003, Stürzl and Zeil, 2007, Philippides et al., 2011; Narendra et al., 2013; Stürzl et al.,
51 2015). This minimum provides a measure of familiarity in addition to a heading direction
52 (Baddeley et al., 2011, 2012; Graham et al., 2010).

53 Before becoming foragers, ants perform a series of learning walks around the nest during
54 which they alternate between turning to look in the nest direction (Müller and Wehner, 2010;
55 Fleischmann et al., 2016, 2017, 2018a,b) and in directions away from the nest from different
56 compass directions (Jayatilaka et al., 2018; reviewed in Zeil and Fleischmann, 2019). It is
57 attractive to assume that the ants store snapshots during these turns whenever they are
58 aligned parallel to the home vector, that is, when they are facing toward or away from the
59 nest direction (Wehner and Müller, 2010; Graham et al., 2010; Jayatilaka et al., 2018), as this
60 is theoretically sufficient for returning ants to align with and walk into the direction of the
61 most familiar of nest-directed snapshots in order to pinpoint the nest (Graham et al., 2010;
62 Baddeley et al., 2012; Wystrach et al., 2013).

63 Such visual 'alignment matching' (Collett et al., 2013) explains well how ants recover the
64 correct direction when on their familiar route (Wystrach et al., 2011b; Wystrach et al., 2012;
65 Baddeley et al., 2012; Kodzhabashev and Mangan, 2015). Moreover, nest-directed views
66 acquired during learning walks (reviewed in Collett and Zeil, 2018; Zeil and Fleischmann, 2019)
67 can also provide guidance from locations that are unfamiliar to ants and that can be 10-15m
68 away from the nest in open forest habitats (Narendra et al., 2013; Stürzl et al., 2015), although

69 the initial movements of released ants may not be directed toward the nest (Zeil et al., 2014),
70 but toward a familiar route (Collett et al., 2007; Wystrach et al., 2012).

71 Overall, this line of work has led to the suggestion that visually navigating insects would only
72 need ‘procedural knowledge’ about knowing where to go rather than requiring a more
73 sophisticated representation of their spatial environment that would allow them ‘to know
74 where they are’ (Collett et al., 2002; Wehner et al., 2006; Cheung et al., 2014; Graham and
75 Philippides, 2017).

76 To test this directly, we positioned ants that we had tethered over a trackball at different
77 locations in their natural foraging environment, including above their nest, and recorded their
78 intended direction and distance of movement. Ants mounted on the ball were well oriented
79 towards the nest at both on and off route locations, but displayed a search pattern when
80 above the nest, as if they knew they were at the nest, implying a sort of positional rather than
81 just procedural knowledge. Using a simple agent-based-simulation we show, however, that
82 these results can be more parsimoniously explained by alignment matching involving
83 continuous integration of attractive and repellent visual memories, acquired when facing
84 respectively towards and away from the nest during learning walks.

85

86 Materials and Methods

87 *Ants and experimental site*

88 We worked with foragers of the Australian Jack Jumper ant *Myrmecia croslandi* from a nest
89 in the Australian National University’s campus field station ($-35^{\circ} 16' 49.87''S$ and $149^{\circ} 06'$
90 $43.74''E$). The ants are day-active, visually navigating solitary foragers that hunt for insects on
91 the ground at up to 4 m distance from the nest and on trees, about 12 m away from the nest
92 where they also feed on sugar secretions of plant-sucking insects (see centre panel top row,
93 Fig. 2). For details of the foraging ecology and the navigational abilities of these ants see
94 Jayatilaka et al. (2011, 2014), Narendra et al. (2013) and Zeil et al. (2014). During February to
95 March 2017 and December 2017 to March 2018, between 9:00 and 15:00, we caught foraging
96 ants either at their foraging trees about 12 m from the nest in a ‘full vector’ state (FV, $n=10$)
97 or at the nest in ‘zero vector’ state (ZV, $n=18$), offered them sugar water solution to feed on

98 before immobilizing them on ice for up to 15 min and tethering them to a metal pin by their
99 mesonotum (thorax) using Bondic liquid plastic welder (Biochem Solutions, Eilerslie, New
100 Zealand). The ants were placed on an air-cushioned light-weight, 5 cm diameter track ball (Fig.
101 1A) on which they were free to rotate around the yaw axis but that allowed us to record their
102 intended translational movements as described in detail by Dahmen et al. (2017). We placed
103 the trackball contraption with a tethered ant at each of three locations in a random order
104 (Fig. 2, top row centre panel): 6.5 m west of the nest where none of the ants were likely to
105 have been before (Off-route), 6.5m south of the nest, half-way along their normal foraging
106 route towards trees (On-route), and directly above the nest (Nest).

107 We recorded the intended movement directions and distances on the trackball at each
108 displacement for up to 10 minutes, before shifting the track ball contraption together with
109 the tethered ant to the next location. Ants were carefully un-tethered and released close to
110 the nest following the three displacements.

111 To demonstrate the foraging patterns of ants at this nest and the full range of learning walks,
112 we show the paths of foraging ants, ants that performed learning walks and ants that were
113 released after contributing to unrelated experiments that were recorded with Differential
114 GPS over two years (Fig. 2, top row centre panel and Fig. S1; for details see Narendra et al.,
115 2013). In brief, coloured flag pins were placed on the ground approximately 20 cm behind a
116 walking ant at fairly regular intervals, carefully avoiding disturbing her progress. The resulting
117 pin trail was subsequently followed with the rover antenna of a Differential GPS system,
118 recording the position with an accuracy of better than 10 cm.
119

120 *Data analysis*

121 We recorded trackball rotations due to the intended translation of the ants at 275 fps, which
122 reflect the direction and speed of the ants' intended movements. We present the
123 reconstructed paths, final bearings, changes in walking direction and path lengths for the first
124 5 min of recordings at the three displacement locations. With the exception of one ant at the
125 off-route location, all ants reached this criterion. We used the Matlab (MathWorks, Natick,
126 MA, USA) circular statistics toolbox (by Philipp Berens) to perform Rayleigh's test for non-
127 uniformity on directional data and Wilcoxon Rank Sum tests on differences between
128 displacement locations using the ranksum function in Matlab. For comparisons between all

129 three locations we applied a Bonferroni correction with a resulting critical value for individual
130 tests of $p=0.0167$.

131

132 *Agent-based modelling*

133 Reconstructed world and ant views: We rendered panoramic views within a 3D model of the
134 ants' natural environments that was previously reconstructed at the ANU Campus Field
135 Station using a laser scanner and camera-based methods (Stürzl et al., 2015). We down-
136 sampled the rendered views to 360×180 pixels, that is, $1^\circ/\text{pixel}$ resolution to roughly match
137 the resolution of the ants' compound eyes. Note that the 3D model was obtained 3 years
138 before the treadmill experiments were conducted, so that there will be some changes to the
139 landmark panorama, in particular involving the canopy, while all the major geometric
140 relationships of dominant visual features such as trees will have remained the same.

141 Memorised views and current familiarity: The agent is assumed to have stored a collection of
142 memorised views around the nest during learning walks and along their normal foraging route
143 (Fig. 1B). During tests, the agent is computing a value of visual familiarity at each time step by
144 comparing the current view to its memory bank. This is achieved by calculating the global root
145 mean squared pixel difference (Zeil et al., 2003) between the current view and each of the
146 views in the memory bank, and keeping the value of the lowest mismatch, as is typically done
147 in models and studies of ant navigation (Wystrach et al., 2011b; Wystrach et al., 2012;
148 Baddeley et al., 2011, 2012; Philippides et al., 2011; Narendra et al., 2013, Zeil et al., 2014,
149 Stürzl et al., 2015). Because high mismatch values indicate a large discrepancy between the
150 current and a memorized view, the value indicates the current unfamiliarity score rather than
151 a familiarity score. Note that in the insect brain, the activity of the mushroom body output
152 neurons (MBON) also correlate with unfamiliarity rather than familiarity (Owald et al., 2015;
153 Felsenberg et al., 2018). Importantly, views in this model are not rotated, but compared only
154 at the facing direction of the current and memorized views. That is, the agent does not need
155 to stop and scan because only one view is compared for each step.

156 Combining attractive and repellent visual memories: The novel aspect of this current model
157 is that the agent is assumed to have two independent memory banks (Fig. 1B-D): one
158 containing attractive views and one containing repellent views. Both memory banks contain

159 views experienced during learning and foraging walks; the attractive memory bank containing
 160 views that are assumed to have been memorised when the ants were oriented toward the
 161 nest and the repellent memory bank those that have been memorised while looking away
 162 from the nest. This is motivated by the very regular scanning movements of ants during their
 163 learning walks where they alternate looking towards the nest and away from the nest
 164 direction (Jayatilaka et al., 2018; Zeil and Fleischmann, 2019). For simplicity, learning walk
 165 views were assumed to have been acquired within a 1 m radius around the nest and we chose
 166 a 10 m long route, corresponding roughly with the foraging corridor of this particular nest
 167 (see Fig. 2, top centre panel). Both nest-directed (attractive) learning walk views and views
 168 away from the nest (repellent) were taken from positions along a spiral rather than a circle
 169 around the nest (Fig. 1B), to mimic the fact that successive learning walk loops reach
 170 increasing distances from the nest (e.g. Fleischmann et al., 2016; Jayatilaka et al., 2018) and
 171 to ensure that results at the nest were not dependent on having views memorised at the
 172 exact same distance from the nest. We also included in the attractive memory bank views
 173 that foragers experience when travelling back to the nest along their normal foraging corridor
 174 (Fig. 1B).

175 Modelling procedure: At each time step, the agent computes two values of unfamiliarity: one
 176 by comparing the current view to the attractive memory bank and one by comparing the same
 177 current view to the repellent memory bank (Fig. 1C & D). These two unfamiliarity values are
 178 assumed to have an antagonistic effect on the agent's behaviour by turning it towards
 179 attractive and away from repellent stimuli with the balance between the two drives
 180 determining the agent's turning direction. We modelled this by a simple subtraction resulting
 181 in a raw overall drive

$$182 \text{ Raw overall drive} = (\text{attractive unfamiliarity value} - \text{repellent unfamiliarity value}) / 0.2 \quad (1)$$

183 We normalised the value of this drive by using always the same value (0.2 in our world),
 184 corresponding roughly to the unfamiliarity score obtained between views from locations in
 185 the virtual world that are far apart, so that *Raw overall drive* will be contained between -0.5
 186 and 0.5. A negative value thus indicates that 'attractive unfamiliarity' < 'repellent
 187 unfamiliarity'. A positive value indicates that 'attractive unfamiliarity' > 'repellent
 188 unfamiliarity'. We then transform *Raw overall drive* into an *Overall drive* with values ranging
 189 from 0 to 1 using a simple sigmoid function:

$$190 \quad \text{Overall drive} = \text{Sigmoid}(\text{Raw overall drive}) \quad (2)$$

191 As a result, the *Overall drive* tends towards 0 if ‘attractive unfamiliarity’ < ‘repellent
 192 unfamiliarity’, towards 1 if ‘attractive unfamiliarity’ > ‘repellent unfamiliarity’ and is 0.5 if
 193 ‘attractive unfamiliarity’ = ‘repellent unfamiliarity’. In other words, a low score indicates that
 194 the current view matches a view in the attractive memory bank better than in the repellent
 195 memory bank and a high score indicates that the current view matches a view in the repellent
 196 memory bank better than in the attractive memory bank (Fig. 1C).

197 To drive the agent, we used a similar approach to Kodzhabashev and Mangan (2015). The
 198 agent is a simple dot in space (x,y) with a current heading (theta). The agent has a
 199 continuously running oscillator alternating between left mode and right mode, which controls
 200 the current turning direction. For simplicity, we modelled this by simply alternating the
 201 turning direction at each time step (Left-Right-Left-Right) as in Kodzhabashev and Mangan
 202 (2015). The resulting paths typically show sharp zigzags, however it is worth noting that
 203 alternating turning direction every 4th step produces smoother oscillations that better
 204 resemble real ant paths (Fig. 1E).

205 *Turn direction* is thus purely controlled by the oscillator, however, the *Turn amplitude* is
 206 directly dependent on the current *Overall drive* (see previous section), that is, on the current
 207 view familiarities.

$$208 \quad \text{Turn amplitude (deg)} = \text{gain} \times \text{Overall drive} \quad (3)$$

209 We use a single parameter (gain) to convert the *Overall drive* (between 0 and 1) into the
 210 angular value for the turn amplitude. We simply used gain = 180, so that the turning amplitude
 211 would vary between 0 degrees (if *Overall drive* = 0) and 180 degrees (if *Overall drive* = 1), with
 212 90 degrees if *Overall drive* = 0.5, that is if attractive and repellent unfamiliarity values are
 213 equal.

214 Across time steps (n), the agent orientation (theta) will thus alternate between left and right
 215 turns ((-1)ⁿ), with each turn varying between 0 and 180 degrees.

$$216 \quad \text{Theta}(n+1) = \text{Theta}(n) + (\text{Turn amplitude} \times (-1)^n) + \text{noise}$$

217 To ensure that the agent is robust against the intrinsic noise of the real world, we added noise
218 at each time step, as a random angular value drawn from a Gaussian distribution ($\mu=0$;
219 $\text{std}=10$ degrees).

220 Agent on a fictive tread-mill: We simulated agent behaviour on a fictive treadmill by simply
221 preventing forward motion. That is, at each time step we assumed that the agent (1) obtains
222 the current view and computes its *Overall drive* (Eqn 1 & 2); (2) turns on the spot with turn
223 direction determined by the state of the oscillator and turn amplitude by Eqn 3 & 4. Since the
224 location at which the agent is standing does not change, the view perceived at each time step
225 only varies depending on the agent's current orientation. The agent on the tread mill was
226 tested at different release locations and we recorded the resulting behaviour.

227 Using attractive visual memories only: We also tested the agent using the attractive memory
228 bank only. In that case

229 *Raw overall drive = attractive unfamiliarity/0.2 - 0.5.*

230 Given that attractive unfamiliarity is always positive, we removed 0.5 during normalisation to
231 centre the *Raw overall drive* on 0, ranging roughly from -0.5 to 0.5 in the same way as when
232 combining attractive and repellent memories. We then used the same sigmoid function to
233 obtain an *Overall drive* between 0 and 1 (Eqn 2).

234

235 Results

236 *Myrmecia ants released on the tread-mill*

237 Irrespective of whether they were caught in a zero-vector state (ZV) or a full-vector state (FV),
238 tethered ants behaved differently when placed 6.5 m west of the nest (off-route, Fig. 2, top
239 left panel), 6.5 m south of the nest (on-route, Fig. 2, bottom middle panel) or over the nest
240 (Nest, Fig. 2, top right panel).

241 In the off-route and on-route locations, most intended paths of both ZV and FV ants were goal
242 directed either to the nest or to the individuals' specific foraging trees (see inset circular
243 histograms in Fig. 2). This is to be expected for *M. croslandi* foragers, which ignore path
244 integration information in the FV state as long as the landmark panorama provides

245 navigational information (see Narendra et al., 2013; Zeil et al., 2014). The paths tended to be
246 straight (see Fig. 3D). In contrast, over the nest, ZV ants moved in random directions, while
247 FV ants tended to move roughly along the home vector direction to the north (at 90° Fig 2,
248 black tracks, top right panel, see also Fig. 3B). Both ZV and FV ants at the nest changed their
249 walking direction frequently. Inset histograms show that most tethered ants over the nest
250 ended up after 5 minutes at final virtual distances less than 10 m from the nest (median 6.07
251 m), while at the on-route location, most ants reached much larger virtual distances (median
252 12.61 m) in the same amount of time (Wilcoxon Rank Sum test: nest vs on-route distances
253 are different: $p = 0.0045$; $z = 2.8378$. See Fig. S2A). The median distances reached at the off-
254 route location are not larger than the ones at the nest (median 6.2 m), owing to a conspicuous
255 peak at small distances contributed by ants that were lost at this location.

256 The behaviour of ants at the off-route location is interesting primarily because most ants are
257 home directed despite it being unlikely that they have ever been to this location before (see
258 inset circular histogram, Fig. 2, top row left panel). A heat map of the foraging movements of
259 124 ants from this nest that had been DGPS-tracked on their outward foraging trips over two
260 years shows that no ant had moved off-route of the nest for more than a few meters (Fig. 2,
261 top row middle panel). Some of the tethered ants appear to have headed towards their
262 foraging trees or the foraging corridor in south-easterly direction, however, when we track
263 ants that were released just north of the off-route location, many initially for 2 m or so do
264 walk in a south-easterly direction before turning east toward the nest (Fig. 2, bottom row, left
265 panel). Tethered ants at the off-route location must therefore get their bearing by comparing
266 what they currently see with nest-directed views they are likely to have gathered during their
267 learning walks, which can extend up to 4 m from the nest (Fig. 2, bottom right panel. See also
268 Jayatilaka et al., 2018).

269 Both FV and ZV ants at the on-route location decided to move either back toward the nest or
270 south toward their foraging trees (Fig. 2, bottom row, centre panel). Otherwise, they moved
271 in a similar way than when at the off-route location. Most of them moved fast, straight and
272 for distances far exceeding those needed to reach the nest or the trees.

273 The most conspicuous feature of paths at the nest location is the fact that the initial walking
274 direction of ZV ants is random, while those of FV ants is in the general home vector direction
275 (north) and that both ZV and FV ants change walking direction frequently.

276 We quantify these differences between locations in three ways in Fig. 3, considering final
277 bearings, the relationship between path length and distance reached and changes in walking
278 direction. Fig. 3A shows the initial paths of ants at the three locations in more detail to
279 emphasize the different behaviours and to highlight the additional fact that paths are fairly
280 smooth at the off-route and on-route locations, but show a distinct sinusoidal oscillation at
281 the nest location. With the exception of the bearings of ZV ants at the nest (Fig. 3C right panel)
282 and those of FV ants after 5 min at the off-route and the nest location (Fig. 3C left and right
283 panel) the virtual bearings of ants after 5 minutes or at 5 m distance from the start are all
284 significantly different from uniform distributions, both for ZV (Fig. 3B) and FV ants (Fig. 3C).
285 While the distributions are unimodal for the off-route and nest location (see insets Fig. 3B
286 and C for circular statistics), they are clearly bimodal at the on-route location.

287 One measure of the straightness of paths is the way in which the straight-line distance from
288 the start depends on path length (Fig. 3D), with straight paths without changes in direction
289 lying close to the line of equality. After 5 minutes, the distribution of the ratios of final
290 distance to final path length differs between the sites (see insets in Fig. 3D and Fig. S2B) with
291 the on-route paths being significantly straighter with a median ratio of distance over path
292 length of 0.83, compared with 0.62 at the off-route location and of 0.45 at the nest location
293 (Wilcoxon Rank Sum test at 5% significance level: On-route vs off-route: $p=0.0110$; on-route
294 vs nest: $p=8.4992e^{-4}$; off-route vs nest: $p = 0.6$. See Fig. S2B).

295 Finally, the behaviour of ants at the three sites also differs on a finer scale: the distribution of
296 changes in path direction is much broader at the nest site, compared to the off-route and on-
297 route location (Fig. 3E) reflecting the conspicuous oscillations of ant paths over the nest (see
298 right panel, Fig. 3A). Note that these distributions have very long tails due to spikes of very
299 high angular velocities which may be artefacts of trackball rotations when the ants are moving
300 very slowly (see time series in Fig. 4). To test whether changes in path direction are indeed
301 systematically larger at the nest location, we calculated the means of their absolute values at
302 11fps over the first 5 min of walking for each ant and compared their distributions, both for
303 angular velocities smaller than $200^\circ/s$ (insets Fig. 3E and Fig. S2C) and for all angular velocities
304 (Fig. S2D). Below $200^\circ/s$, nest paths are indeed wigglier compared to on-route paths (Fig. S2C,
305 Wilcoxon Rank Sum test: nest vs on-route $p=2.56e^{-4}$, $z=-3.6563$), with the difference between
306 nest and off-route location just failing to reach significance (nest vs off-route $p=0.019$, $z=-$

307 2.3458). Considering the whole range of angular velocities (Fig. S2D) there is no difference
308 between nest and the other locations, mainly because of high angular velocities exhibited by
309 ants at all sites.

310 We note that many ants at various times during the first 5 minutes on the trackball over the
311 nest show very regular path oscillations as documented in Fig. 3A and for three examples in
312 Fig. 4 (red traces). The distribution and the time course of changes in path direction over the
313 nest are different from those exhibited by the same ants at the on-route location (shown in
314 blue in Fig. 4). Regular and sustained path oscillations lead to periodicities in the auto-
315 correlation function of changes in path direction and can be detected in 13 out of 25 cases of
316 ants participating in all three locations (blue traces in Fig. S3), compared to 4/25 at the off-
317 route location (red traces in Fig. S3) and 1/25 at the on-route location (green traces in Fig.
318 S3). We add the caveat that the statistics of path properties are unlikely to be stationary
319 during an experiment and that this particular aspect of ant behaviour will require future
320 attention.

321

322 *Agent-based modelling*

323 To model the agent on a fictive tread-mill, we simply prevented it from stepping forward, so
324 that views were always perceived from the same spot, and where rotated according to the
325 agent's current facing direction. We released the agent at four locations.

326 When tested close to the beginning of the homing route (on-route RP), the agent oriented
327 mostly in the correct direction, that is, along the route towards the nest (blue paths in Fig.
328 5A). This is because the overall drive is close to 0 while facing in this direction (the attractive
329 unfamiliarity is very low and the repellent unfamiliarity is high (Fig. 1C) yielding very small
330 turns (Fig. 5B & C). Note that if the agent happened to face in the opposite direction (due to
331 noise), the overall drive would strongly increase and thus trigger a large turn.

332 When released away from the route (off-route RP), the agent also favoured one direction
333 indicating that this direction provided a smaller overall drive (yellow paths in Fig. 5A). This is
334 an indication that the view at the off-route RP and nest-directed learning walk views are most

335 familiar because their comparison produces a detectable minimum of the rotIDF and that the
336 agent thus favours a direction roughly pointing towards the nest.

337 When released on top of the nest (nest RP), the agent produced convoluted paths with no
338 preferred directions (red paths in Fig. 5A). This is due to the rather uniform distribution of
339 visual familiarities across directions (see Fig. 1C). At a more local scale, the paths show much
340 larger turn amplitudes than at the on-route or off-route RPs (Fig. 5B & C). This is because at
341 the nest location, attractive and repellent memorised views provide a roughly equal match
342 whatever the current facing direction, resulting in an overall drive around 0.5, thus yielding
343 turns that are larger than when attractive and repellent memories match best for different
344 directions (see Fig. 1C).

345 When released at a distant unfamiliar location (distant RP), the agent displayed equally large
346 turn amplitudes as at the nest (marked in black in Fig. 5A-C) because, as for the nest location,
347 both the attractive and the repellent memory bank provide roughly equal unfamiliarity
348 values, thus resulting in an average overall drive around 0.5.

349 In contrast, when using the attractive memory bank only, turn amplitudes were large at the
350 distant unfamiliar location (black) but comparatively low at the nest (red, right column, Fig.
351 5). This is simply because the unfamiliarity value is high in the unfamiliar location (yielding a
352 strong directional drive and thus large turns), and low at the nest due to the good match with
353 learning walks views (yielding a low directional drive and thus small turns).

354

355 *Testing model-predictions with Myrmecia*

356 Motivated by the different simulation results when using 'attractive only' and
357 'attractive/repellent' memory banks as well as by the rather counter-intuitive outcome that
358 the use of 'attractive/repellent' memories predicts a similar behaviour at the familiar nest
359 location and at a completely unfamiliar location, we released *Myrmecia* ants mounted on the
360 trackball both at the nest and at a distant location about 50 m south-west of the nest. The
361 location was far beyond the ants' foraging trees and thus was likely to be completely
362 unfamiliar to the ants. Strikingly, ants at this distant release location behaved in a similar way
363 as at the nest, both in terms of the ratio between the distance reached after 5 minutes and

364 the path length (see box plot insets in Fig. 6A centre panels, Wilcoxon Rank Sum test
365 unfamiliar vs nest location: $p=0.7984$, ranksum=71) and in terms of the mean absolute
366 changes in walking direction (see box plot insets in Fig. 6A right panels, Wilcoxon Rank Sum
367 test unfamiliar vs nest location: $p=0.9591$, ranksum=67). The ants at both the unfamiliar and
368 the nest site also displayed the characteristic path oscillations we observed at the nest in our
369 previous experiments (Fig. 6A and B, compare with Fig. 4), as predicted by the
370 attractive/repellent model.

371

372 Discussion

373 Our behavioural experiments revealed three fundamental properties of visual navigation in
374 ants that could only be uncovered using the trackball method. First, we determine that
375 whether on-route or off-route, several metres away from the nest, ants can recover the goal
376 direction without the need to physically move and to sample neighbouring locations. Second,
377 we find no evidence that they 'expect' outcomes from their behaviour, such as a changing
378 visual scene or increasing certainty about the location of the nest. *M. croslandi* ants show no
379 evidence of monitoring the distance that separates them from the goal, unlike for instance
380 ants that rely strongly on path integration (Dahmen et al., 2017). Third, ants behave
381 differently when positioned above the nest, by following random heading directions and
382 frequently changing their walking direction. These are the characteristics of search behaviour
383 and thus could be interpreted as indicating that ants 'know' that they are at the nest, as if
384 they possessed location information. However, our simulation results demonstrate that the
385 nest-specific behaviour of ants can be parsimoniously explained by the density of attractive,
386 nest-directed, and repellent views away from the nest that at least *M. croslandi* ants are likely
387 to acquire in the course of systematic scanning movements during their learning walks (e.g.
388 Jayatilaka et al., 2018). Our simulation also confirms that the same parsimonious mechanism
389 can recover a correct direction from on- and off-route locations, as previous modelling has
390 indicated (Baddeley et al., 2011, 2012; Narendra et al., 2013; Wystrach et al., 2013;
391 Kodzhabashev and Mangan, 2015).

392

393 *Alignment matching and visual memories*

394 Current thinking holds that ants during their learning walks learn nest-directed views
395 (*Cataglyphis sp*: Fleischmann et al., 2016, 2017, 2018a,b; *Ocymyrmex robustior*: Müller and
396 Wehner, 2010; *Melophorus bagoti*: Wehner et al., 2004; Muser et al., 2005) and possibly both
397 nest-directed views and views pointing away from the nest (*Myrmecia croslandi*: Jayatilaka et
398 al., 2018; Zeil and Fleischmann, 2019). In addition, they memorize the views they experience
399 along routes as they go back and forth on foraging excursions (Wehner et al., 1996; Mangan
400 and Webb, 2012; Kohler and Wehner, 2005; Wystrach et al., 2010; Freas and Specht, 2019).

401 When using their visual memories to navigate, the currently perceived panorama provides a
402 heading direction if the comparison between memorised views and the current view
403 generates a detectable minimum of the rotational image difference function (see Narendra
404 et al., 2013). This is a basic measure of familiarity and at any location, the direction presenting
405 the most familiar view would provide the deepest (lowest) minimum. At both the on-route
406 and off-route location ants on the trackball were free to scan the panorama and detect the
407 direction of any present minima. Our results show that they were successfully able to recover
408 the goal direction by doing so (Fig. 2). On route, some ants headed to the nest while others
409 aimed at their foraging trees, reflecting their motivation to home or to forage.

410 While the directedness of ants at the on-route site would have been supported by both
411 learning walk views and views learnt along the route, their directedness at the off-route
412 (west) location depends on their detecting a higher similarity with learning walk views
413 directed at the nest from the west compared to all other nest-directed views. As shown here
414 and before (Narendra et al., 2013; Zeil et al., 2014; Stürzl et al., 2015), this is possible up to
415 10-15m distance from the nest in the open woodland habitats of *Myrmecia* ants, provided
416 ants have acquired such nest-directed views about 1 to 5 metres away from the nest (see Fig.
417 2B, bottom right).

418 When released at the nest, ants behaved differently. They walked in various directions and
419 displayed larger turns that regularly alternated between left and right, resulting in sinusoidal
420 paths. So are nest views special?

421 As far as navigational information is concerned, the situation at the nest is indeed different
422 compared with both on- and off-route sites. During their learning walks ants will have

423 encountered a dense set of views at different distances and compass bearings around the
424 nest, each potentially tagged with the nest direction through path integration (Müller and
425 Wehner, 2010; Graham et al., 2010; Baddeley et al., 2012; Fleischmann et al., 2018a;
426 Jayatilaka et al., 2018; Zeil and Fleischmann, 2019). In contrast to other locations, tethered
427 ants placed above the nest location thus will encounter attractive familiar views (or deep
428 rotIDF minima) in many compass directions, which might explain why they initially walked in
429 various directions at this location.

430 The high amplitude oscillation displayed by ants at the nest location, however, is puzzling.
431 Previous models suggest that experiencing a familiar (attractive) view should inhibit turns and
432 favour forward motion (Zeil, 2012; Möller, 2012; Baddeley et al., 2011, 2012; Wystrach et al.,
433 2013; Kodzhabashev and Mangan, 2015; Ardin et al., 2016), which is here clearly not the case.
434 The behaviour of tethered ants on top of the nest can be interpreted as search for the nest
435 entrance, which in ants relying on path integration is characterized by frequent changes in
436 path direction and a systematic pattern of increasing loops around the expected location of
437 the goal (e.g. Schultheiss et al., 2015). To our knowledge, however, no analysis of the fine-
438 scale changes in orientation of searching ants – as we observed them here - has been done
439 to date.

440 Previous work has suggested that the recognition of views memorised at the nest may trigger
441 specific behaviours when subsequently released in unfamiliar locations (Wystrach et al.,
442 2013). This interpretation may suggest positional knowledge, or at least that views close to
443 the nest are categorised separately from route views during learning and being treated
444 differently when recognised. In the following we discuss the results of our simulation that
445 suggest a parsimonious and unifying explanation for view-based route guidance, pinpointing
446 goals and the current observation of high amplitude oscillation at the nest without the need
447 to invoke positional knowledge or the need for a ‘trigger’ of search behaviour. Our agent-
448 based modelling exhibits the same pattern of fine-scale oscillations, including overall changes
449 in path direction, but only if we assume that the agent operates with both attractive and
450 repellent memory banks.

451

452 *Continuously integrating attractive and repellent views*

453 Our model was developed quite independently to explain other recently observed
454 phenomena, such as how ants manage to use views for guidance while walking backward and
455 thus facing in the anti-nest direction (Schwarz et al., under review); or how ants learn to
456 detour areas along their route associated with an aversive experience (Wystrach et al., 2019).
457 Interestingly, this new model happens to also capture the current results remarkably well.
458 The model is based on two assumptions: (1) that ants store both attractive and repellent
459 views during their learning walks as suggested by Jayatilaka et al. (2018), and (2) that guidance
460 involves an oscillator resulting in a continuous alternation between left and right turns
461 (Namiki and Kanzaki, 2016; Kodzhabashev and Mangan, 2015; Wystrach et al., 2016). The
462 model assumes no positional knowledge whatsoever, only procedural knowledge.

463 Several pieces of evidence suggest that insects possess an intrinsic oscillator triggering
464 alternatively left and right body rotations, the amplitude of which can be modulated by the
465 stimuli perceived (Namiki and Kanzaki, 2016; Lent et al., 2013; Wystrach et al., 2016). Such a
466 control of oscillations can provide guidance along odour plumes (Namiki and Kanzaki, 2016)
467 and odour gradients (Wystrach et al., 2016), support visual route following (Kodzhabashev
468 and Mangan, 2015) and greatly facilitates the integration of different sources of stimulation
469 (Wystrach et al., 2016). In the case of visual route following, the amplitude of the oscillations
470 needs to be simply modulated by the familiarity of the currently perceived view. The
471 suggestion is that familiar views trigger small turns whereas unfamiliar views trigger large
472 turns, and that the direction of the turn is dependent on the current state of the oscillator.
473 Because views are assumed to be memorized while moving along the route, during route
474 recapitulation visual familiarity is higher when facing in the correct route direction. This model
475 is sufficient for an agent to recapitulate a route in naturalistic environments (Kodzhabashev
476 and Mangan, 2015). However, when released at the nest, this model does not predict large
477 amplitude oscillations such as the ones we observed here in ants. On the contrary, because
478 of the high familiarity experienced at the nest, which results from the collection of nest-
479 oriented views acquired during learning walks, the model predicts an inhibition of the
480 oscillations whatever the current facing direction (see Fig 5, right column).

481 The visual memories used by insect navigators are likely stored in the mushroom bodies
482 (Webb and Wystrach, 2016), but current models assume only the existence of attractive
483 memories (Möller, 2012; Baddeley et al., 2011, 2012; Wystrach et al., 2013; Kodzhabashev

484 and Mangan, 2015; Ardin et al., 2016). Here we incorporated into the model the recent
485 suggestion that ants store both attractive and repellent views, mimicking the so-called
486 'appetitive/aversive' output pathways from the insect mushroom bodies (e.g. Oswald et al.,
487 2015; Saumweber et al., 2018) (Fig. 1D). Indeed, during their learning walks, many ants, not
488 only *Myrmecia croslandi* (Jayatilaka et al., 2018) display regular head and body oscillations,
489 facing alternatively towards and away from the nest (Zeil and Fleischmann, 2019). We
490 assumed in our model that these views form two distinct memory banks: one holding
491 'attractive', nest-directed, views and one holding 'repellent' views pointing away from the
492 nest, and that both sets are used continuously and simultaneously during homing. Our agent
493 compares the current view to both sets of memories at each time step and thus obtains two
494 familiarity values, one for attraction (high familiarity, inhibiting turns) and one for repulsion
495 (high familiarity, triggering large turning amplitudes). Given that both memory pathways have
496 antagonist outcomes, they can be simply integrated by subtracting attractive and repellent
497 familiarity values, resulting in what we called here an 'overall drive' which modulates the
498 amplitude of the oscillator (Fig. 1C).

499 Interestingly, this model closely mimics ant behaviour as documented in our behavioural
500 experiments. If released on a fictive tread-mill (preventing the agent from translating) it
501 displays high amplitude turns when released on top of the nest, and much lower amplitude
502 turns when released further along the homing route. In contrast, when using the 'attractive'
503 memory bank only, the agent produces low amplitude turns at the nest (Fig 5).

504 The behaviour of the agent when combining attractive and repellent views is straightforward
505 to explain (Fig. 1C). At the route release point, facing in the correct direction the simulation
506 generates very small turns because only the attractive memory bank provides a good match.
507 By integrating this with a high unfamiliarity of the repellent memory bank, we obtain a very
508 low overall drive, and thus small turns. However, when released at the nest, whatever the
509 direction the agent faces, there are always both attractive and repellent views that are
510 matching the current view (Fig. 1C). The reason being that these views, when acquired during
511 learning walks, are experienced in multiple compass direction at very closely spaced locations
512 (Fig. 1B). Both attractive and repellent pathways signal high familiarity values and cancel each
513 other out, resulting in large turns.

514

515 *Testing the model's prediction.*

516 Interestingly, the attractive/repellent memory bank model makes a rather counterintuitive
517 prediction, because it relies on the relative difference in familiarities between attractive and
518 repellent pathways and not on the absolute familiarity experienced: the agent's behaviour
519 should be similar when on top of the nest and at a completely unfamiliar location, outside the
520 catchment area of acquired views. At the nest, both attractive and repellent memories result
521 in high familiarity, so their signals cancel each other when integrated (attractive - repellent),
522 resulting in large turns. In completely unfamiliar terrain, both attractive and repellent
523 memories result in very low familiarity, and thus their signals equally cancel each other when
524 integrated (attractive - repellent), resulting also in large turns (Fig. 1C).

525 As predicted by the model, experiments showed indeed that ants tethered at a completely
526 unfamiliar location exhibit a very similar behaviour to when released on top of the nest: that
527 is, they displayed regular high amplitude path oscillations (Fig. 6).

528

529 *Integration with path integration.*

530 We did not incorporate integration of path integration information and landmark panorama
531 guidance in our model and so do not at this stage tackle the fact that full vector ants (i.e.,
532 those captured with a remaining path integration home vector) showed a small bias towards
533 the home vector direction at the nest location (Fig. 2 & 3, FV vs ZV ants). In *M. croslandi*
534 foragers, as in other ants, path integration information and scene information are integrated
535 (Collett et al., 2001; Collett, 2012; Reid et al., 2013 ; Legge et al., 2012; Narendra et al., 2013;
536 Wystrach et al., 2015; Wehner et al., 2016) with familiar views more strongly weighted – to
537 the degree that a current view providing information on heading direction can completely
538 override conflicting information from path integration (Kohler and Wehner, 2005; Narendra
539 et al., 2013; Zeil et al., 2014). In ants that rely heavily on path integration, this information is
540 more strongly weighted as the length of the vector increases (Wystrach et al., 2015; Wystrach
541 et al., 2019). The bias towards the home vector direction observed here in FV ants fits this
542 current view, which is summarised in a recent model (Hoinville and Wehner, 2018). Also,
543 experienced ants seem to rely less on path integration than naïve ants, and rather display a

544 search when on unfamiliar terrain (Schwarz et al., 2017), which may explain why path
545 integration information is never strongly weighted in the long-lived *M. croslandi*.

546

547 Outlook

548 Our results may contribute to the lingering debate about the format of spatial knowledge
549 underlying visual navigation in insects and animals in general (see for instance, Cheeseman et
550 al., 2014a,b and Cheung et al., 2014; Warren, 2019). We showed that ants released on top of
551 the nest displayed large turns. These results were clearly at odds with the current ‘procedural’
552 models, stipulating that the high familiarity of views at the nest should inhibit turns. In
553 contrast, the ants’ behaviour suggested that they could derive positional knowledge from the
554 current views, given the interpretation that the ants searched because they recognised that
555 they were at the nest. Previous results, such as the apparent ability of insects to make
556 shortcuts also favoured explanations assuming ‘positional’ rather than ‘procedural’
557 knowledge (e.g. Cheeseman et al., 2014a,b; Warren, 2019). However, as often in the insect
558 literature (Cartwright and Collett, 1983; Collett et al., 2007; Cruse and Wehner, 2010;
559 Wystrach and Graham, 2012; Narendra et al., 2013; Cheung et al., 2014), an alternative, more
560 parsimonious explanation can also explain our results: ants may simply combine attractive
561 and repellent memories. Importantly, this procedural explanation did not come from actively
562 seeking for it, but emerged from other observations, such as the way in which ants behave
563 when learning views around the nest (Jayatilaka et al., 2018), avoid adverse situations
564 (Wystrach et al., 2019), steer while walking backwards (Schwarz et al., 2017; Schwarz et al.,
565 under review) as well as how appetitive and aversive memory pathways are combined in
566 other insects such as flies (Felsenberg et al., 2018) and fly larvae (Eichler et al., 2017).

567 Our simulation made the unexpected prediction that behaviour in completely unfamiliar
568 terrain should be the same as at the very familiar nest, which we confirmed by subsequent
569 experimentation. Purely scene familiarity-based modelling replicates these results with
570 astonishing detail, providing support for the suggestion that ants during their learning walks,
571 acquire both attractive, nest-directed views and repellent views when pointing away from the
572 nest during systematic scanning movements (Jayatilaka et al., 2018; Zeil and Fleischmann,

573 2019). It is not clear at present, however, whether all views are memorized irrespective of
574 gaze direction or only when the ants' head is aligned parallel to the home vector (see
575 discussion in Jayatilaka et al., 2018). We show here, at least, that the distinctly different
576 behaviour of ants over the nest location can be replicated if an agent has an attractive and a
577 repellent scene memory bank.

578 The most parsimonious explanation for our observations is therefore that the ants operate
579 on 'procedural' rather than 'location' information (*sensu* Collett et al., 2002; Wehner et al.,
580 2006; Graham and Philippides, 2017): at both familiar and unfamiliar locations away from the
581 nest they may know where to go, but they do not know where they are. Moreover, the main
582 assumptions of our simulation - attractive and repellent view comparison driving an oscillator
583 - can be tested by a detailed comparison of the gaze and path directions of individually
584 identified ants during their learning walks and during their subsequent approach to the nest,
585 when returning from foraging excursions. Such an analysis may also reveal how ants
586 eventually pinpoint the nest entrance, which none of the current homing models can properly
587 explain.

588

589 Acknowledgements

590 We thank Chloé Raderschall and Piyankarie Jayatilaka for tracking ants over the years, Camile
591 Moray, Fiorella Ramirez-Esquivel and Moosarreza Zahedi for help with field work and the
592 mechanical workshop of the Research School of Biology for constructing the housing for the
593 trackball contraption. We are grateful to Marijke Welvaert and Teresa Neeman from the ANU
594 Statistical Consulting Unit for their advice.

595 Competing interests

596 No competing interests declared.

597 Funding

598 We acknowledge financial support from the Australian Research Council, Discovery Project
599 Grant (DP150101172), Future Fellowship (FT140100221), the Hermon Slade Foundation (HSF

600 10/7), the ANU Endowment Fund and the European Research Council (ERCstg: EMERG-ANT
601 759817).

602 **Data availability**

603 Upon acceptance, data will be made available through FigShare. Requests for further
604 information and for original video footage should be directed to and will be fulfilled by the
605 corresponding author, Trevor Murray. Requests for the python code for the model should be
606 directed to Antoine Wystrach.

607 References

- 608 **Baddeley, B., Graham, P., Philippides, A., and Husbands, P.** (2011). Holistic visual encoding
609 of ant-like routes: navigation without waypoints. *Adaptive Behav.* **19**, 3–15.
- 610 **Baddeley, B., Graham, P., Husbands, P., and Philippides, A.** (2012). A model of ant route
611 navigation driven by scene familiarity. *PLoS Comp. Biol.* **8**, e1002336.
- 612 **Baerends, G.P.** (1941). Fortpflanzungsverhalten und Orientierung der Grabwespe
613 *Ammophila campestris*. *Jur. Tijdschrift voor Entomologie* **84**, 68–275.
- 614 **Cheeseman, J. F., Millar, C. D., Greggers, U., Lehmann, K., Pawley, M. D. M., Gallistel, C.**
615 **R., Warman, G. R., and Menzel, R.** (2014a). Way-finding in displaced clock-shifted bees
616 proves bees use a cognitive map. *Proc. Natl Acad. Sci. USA* **111**, 8949-8954.
- 617 **Cheeseman, J.F., Millar, C.D., Greggers, U., Lehmann, K., Pawley, M.D.M., Gallistel, C.R.,**
618 **Warman, G.R., and Menzel, R.** (2014b). Reply to Cheung et al.: the cognitive map
619 hypothesis remains the best interpretation of the data in honeybee navigation. *Proc. Nat.*
620 *Acad. Sci. USA* **111**, E4398.
- 621 **Cheung, A., Collett, M., Collett, T.S., Dewar, A., Dyer, F.C., Graham, P., Mangan, M.,**
622 **Narendra, A., Philippides, A., Stürzl, W., Webb, B., Wystrach, A., and Zeil, J.** (2014). Still
623 no convincing evidence for cognitive map use by honeybees. *Proc. Nat. Acad. Sci. USA*
624 **111**, E4396-E4397.
- 625 **Collett, M.** (2012). How navigational guidance systems are combined in a desert ant. *Curr.*
626 *Biol.* **22**, 927-932.
- 627 **Collett, T.S., and Zeil, J.** (1998). Places and landmarks: an arthropod perspective. In *Spatial*
628 *representation in animals* (ed. S. Healy), pp. 18–53. Oxford, UK: Oxford University Press.
- 629 **Collett, M., Chittka, L., and Collett, T. S.** (2013). Spatial memory in insect navigation. *Curr.*
630 *Biol.* **23**, R789-R800.
- 631 **Collett, M., Harland, D., and Collett, M.** (2002). The use of landmarks and panoramic context
632 in the performance of local vectors by navigating honeybees. *J. Exp. Biol.* **205**, 807-814.

- 633 **Collett, T.S., Collett, M., and Wehner, R.** (2001). The guidance of desert ants by extended
634 landmarks. *J. Exp. Biol.* **204**, 1635–1639.
- 635 **Collett, T. S., Graham, P., and Harris, R.A.** (2007). Novel landmark-guided routes in ants. *J.*
636 *Exp. Biol.* **210**, 2025-2032.
- 637 **Cruse, H., and Wehner, R.** (2011). No need for a cognitive map: decentralized memory for
638 insect navigation." *PLoS Comp. Biol.* **7**, e1002009.
- 639 **Dahmen, H.J., Wahl, V.L., Pfeffer, S.E., Mallot, H.A., and Wittlinger, M.** (2017). Naturalistic
640 path integration of *Cataglyphis* desert ants on an air-cushioned light weight spherical
641 treadmill. *J. Exp. Biol.* **220**, 634-644.
- 642 **Eichler, K., Li, F., Litwin-Kumar, A., Park, Y., Andrade, I., Schneider-Mizell, C.M., Saumweber,**
643 **T., Huser, A., Eschbach, C., Gerber, B., Fetter, R.D., Truman, J.W., Priebe, C.E., Abbott,**
644 **L.F., Thum, A.S., Zlatic, M., and Cardona, A.** (2017). The complete connectome of a
645 learning and memory centre in an insect brain. *Nature* **548**, 175-182.
- 646 **Felsenberg, J., Jacob, P.F., Walker, T., Barnstedt, O., Edmondson-Stait, A.J., Pleijzier, M.W.,**
647 **Otto, N., Schlegel, P., Sharifi, N., Perisse, E., Smith, C.S., Lauritzen, J.S., Costa, M.,**
648 **Jefferis, G.S.X.E., Bock, D.D., and Waddell, S.** (2018). Integration of parallel opposing
649 memories underlies memory extinction. *Cell* **175**, 709-722.
- 650 **Fleischmann, P.N., Christian, M., Müller, V.L., Rössler, W., and Wehner, R.** (2016). Ontogeny
651 of learning walks and the acquisition of landmark information in desert ants *Cataglyphis*
652 *fortis*. *J. Exp. Biol.* **219**, 3137-3145.
- 653 **Fleischmann, P.N., Grob, R., Wehner, R., and Rössler, W.** (2017). Species-specific differences
654 in the fine structure of learning walk elements in *Cataglyphis* ants. *J. Exp. Biol.* **220**, 2426-
655 2435.
- 656 **Fleischmann, P.N., Grob, R., Müller, V.L., Wehner, R., and Rössler, W.** (2018a). The
657 geomagnetic field is a compass cue in *Cataglyphis* ant navigation. *Curr. Biol.* **28**, 1440-
658 1444.

- 659 **Fleischmann, P.N., Rössler, W., and Wehner, R.** (2018b). Early foraging life: spatial and
660 temporal aspects of landmark learning in the ant *Cataglyphis noda*. *J. Comp. Physiol. A*
661 **204**, 579–592.
- 662 **Freas, C.A., and Spetch, M.L.** (2019). Terrestrial cue learning and retention during the
663 outbound and inbound foraging trip in the desert ant, *Cataglyphis velox*. *J. Comp. Physiol.*
664 *A* **205**, 177–189.
- 665 **Graham, P., and Cheng, K.** (2009). Ants use the panoramic skyline as a visual cue during
666 navigation. *Curr. Biol.* **19**, R935–R937.
- 667 **Graham, P., and Philippides, A.** (2017). Vision for navigation: What can we learn from ants?
668 *Arthropod Struct. & Dev.* **46**, 718-722.
- 669 **Graham, P., Philippides, A., and Baddeley, B.** (2010). Animal cognition: multimodal
670 interactions in ant learning. *Curr. Biol.* **20**, R639–R640.
- 671 **Hoinville, T. and Wehner, R.** (2018). Optimal multiguide integration in insect navigation.
672 *Proc. Natl. Acad. Sci. USA* **115**, 2824-2829.
- 673 **Jayatilaka, P., Murray, T., Narendra, A., and Zeil, J.** (2018). The choreography of learning
674 walks in the Australian jack jumper ant *Myrmecia croslandi*. *J. Exp. Biol.*
675 doi/10.1242/jeb.185306
- 676 **Jayatilaka, P., Raderschall, A. C., Narendra, A., and Zeil, J.** (2014). Individual foraging patterns
677 of the jack jumper ant *Myrmecia croslandi* (Hymenoptera: Formicidae). *Myrmecol. News*
678 **19**, 75-83.
- 679 **Jayatilaka, P., Narendra, A., Reid, F.S., Cooper, P., and Zeil, J.** (2011). Different effects of
680 temperature on foraging activity schedules in sympatric *Myrmecia* ants. *J. Exp. Biol.* **214**,
681 2730-2738.
- 682 **Kodzhabashev, A., and Mangan, M.** (2015). Route following without scanning. In *Biomimetic*
683 *and Biohybrid Systems* (ed . S.P. Wilson, P.F.M.J. Verschure, A. Mura and T.J. Prescott),
684 pp. 199–210. *Lecture Notes in Artificial Intelligence 9222*. Heidelberg, Berlin, New York:
685 Springer Verlag.

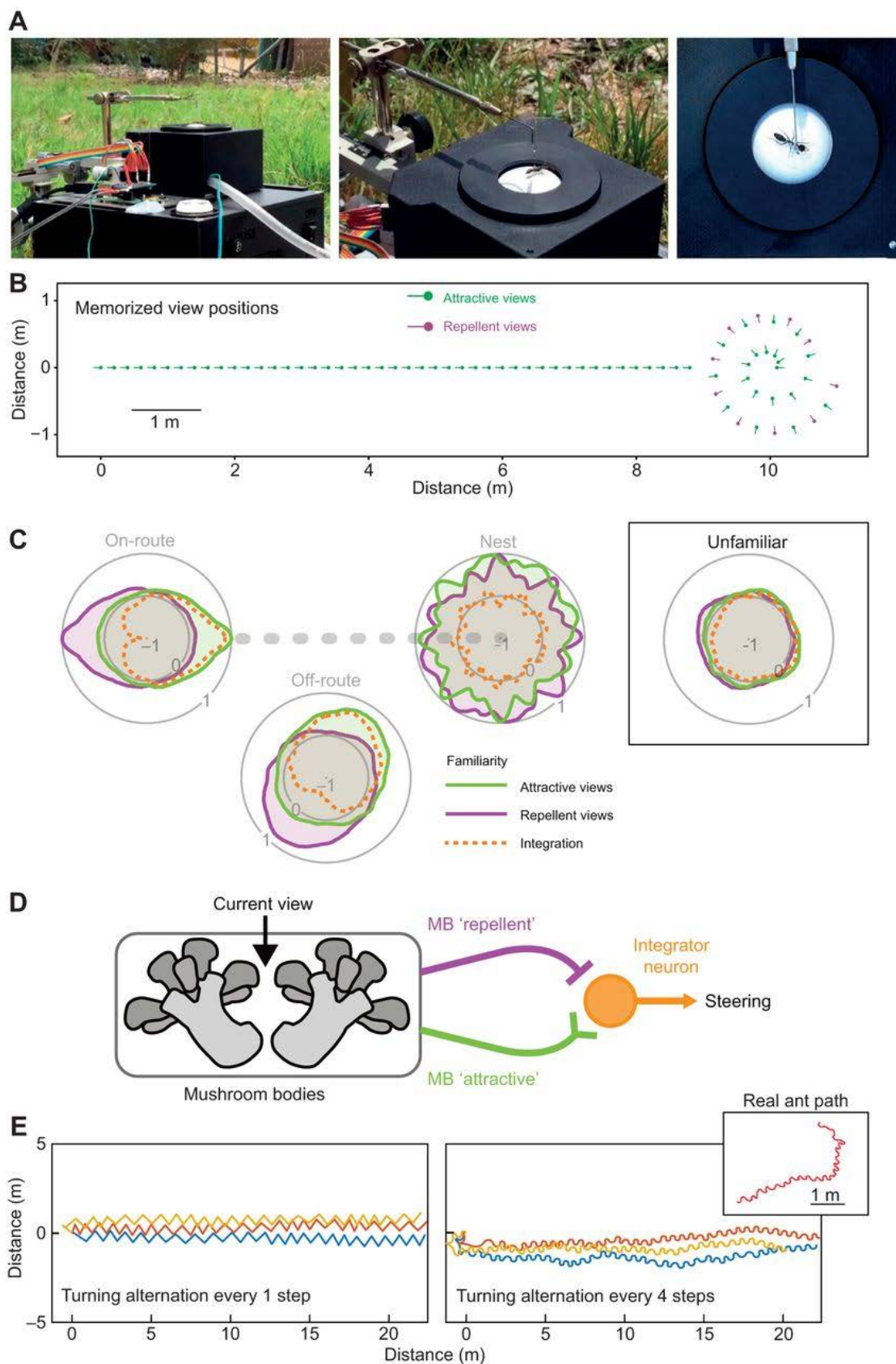
- 686 **Kohler, M., and Wehner, R.** (2005). Idiosyncratic route-based memories in desert ants,
687 *Melophorus bagoti*: How do they interact with path-integration vectors? *Neurobiol.*
688 *Learning and Memory* **83**: 1–12
- 689 **Mangan, M., and Webb, B.** (2012). Spontaneous formation of multiple routes in individual
690 desert ants (*Cataglyphis velox*). *Behav. Ecol.* **23**, 944–954.
- 691 **Möller, R.** (2012). A model of ant navigation based on visual prediction. *J. Theo. Biol.* **305**,
692 118–130.
- 693 **Müller, M., and Wehner, R.** (2010). Path integration provides a scaffold for landmark learning
694 in desert ants. *Curr. Biol.* **20**, 1368–1371.
- 695 **Murray, T., and Zeil, J.** (2017). Quantifying navigational information: The catchment volumes
696 of panoramic snapshots in outdoor scenes. *PLoS ONE* **12**, e0187226.
- 697 **Muser, B., Sommer, S., Wolf, H., and Wehner, R.** (2005). Foraging ecology of the thermophilic
698 Australian desert ant *Melophorus bagoti*. *Austr. J. Zool.* **53**, 301–311.
- 699 **Namiki, S., and Kanzaki, R.** (2016). The neurobiological basis of orientation in insects: insights
700 from the silkworm mating dance. *Curr. Opin. Insect Sci.* **15**, 16–26.
- 701 **Narendra, A., Gourmaud, S., and Zeil, J.** (2013). Mapping the navigational knowledge of
702 individually foraging ants *Myrmecia croslandi*. *Proc. R. Soc. Lond. B* **280**, 20130683.
- 703 **Owald, D., Felsenberg, J., Talbot, C.B., Das, G., Perisse, E., Huetteroth, W., and Waddell, S.**
704 **(2015)**. Activity of Defined Mushroom Body output neurons underlies learned olfactory
705 behavior in *Drosophila*. *Neuron* **86**, 417–427.
- 706 **Philippides, A., Baddeley, B., Cheng, K., and Graham, P.** (2011). How might ants use
707 panoramic views for route navigation? *J. Exp. Biol.* **214**, 445–451.
- 708 **Saumweber, T., Rohwedder, A., Schleyer, M., Eichler, K., Chen, Y.-c., Aso, Y., Cardona, A.,**
709 **Eschbach, C., Kobler, O., Voigt, A., Durairaja, A., Mancini, N., Zlatic, M., Truman, J.W.,**
710 **Thum, A.S., and Gerber, B.** (2018). Functional architecture of reward learning in
711 mushroom body extrinsic neurons of larval *Drosophila*. *Nature Comm.* **9**, 1104.
- 712 **Schultheiss, P., Cheng, K., and Reynold, A.M.** (2015). Searching behavior in social
713 Hymenoptera. *Learning and Motivation* **50**, 59–67.

- 714 **Schwarz, S., Wystrach, A., and Cheng, K.** (2017). Ants' navigation in an unfamiliar
715 environment is influenced by their experience of a familiar route. *Scientific Reports* **7**,
716 14161.
- 717 **Schwarz, S., Mangan, M., Zeil, J., Webb, B., and Wystrach, A.** (2017). How ants use vision
718 when homing backward. *Curr. Biol.* **27**, 401-407.
- 719 **Schwarz, S., Clement, L., Gkaniias, E., and Wystrach, A.** How do backward walking ants
720 (*Cataglyphis velox*) cope with navigational uncertainty? (under review)
- 721 **Stürzl, W., and Zeil, J.** (2007). Depth, contrast and view-based homing in outdoor scenes. *Biol.*
722 *Cybernet.* **96**, 219-531.
- 723 **Stürzl, W., Zeil, J., Boeddeker, N., and Hemmi, J.M.** (2016). How wasps acquire and use views
724 for homing. *Curr. Biol.* **26**, 470–482.
- 725 **Stürzl, W., Grixa, I., Mair, E., Narendra, A., and Zeil, J.** (2015). Three-dimensional models of
726 natural environments and the mapping of navigational information. *J. Comp. Physiol. A*
727 **201**, 563-584.
- 728 **Warren, W.H.** (2019). Non-Euclidean navigation. *J. Exp. Biol.* **222**, jeb187971
- 729 **Webb, B., & Wystrach, A.** (2016). Neural mechanisms of insect navigation. Current opinion in
730 insect science, 15, 27-39.
- 731 **Wehner, R., Michel, B., and Antonsen, P.** (1996). Visual navigation in insects: coupling of
732 egocentric and geocentric information. *J. Exp. Biol.* **199**, 129–140.
- 733 **Wehner, R., Meier, C., and Zolikofer, C.** (2004). The ontogeny of foraging behaviour in desert
734 ants, *Cataglyphis bicolor*. *Ecol. Entomol.* **29**, 240-250.
- 735 **Wehner, R., Boyer, M., Loertscher, F., Sommer, S., and Menzi, U.** (2006). Ant Navigation:
736 One-Way Routes Rather Than Maps. *Curr. Biol.* **16**, 75–79.
- 737 **Wystrach, A., and Graham P.** (2012). What can we learn from studies of insect navigation?
738 *Anim. Behav.* **84**, 13-20.
- 739 **Wystrach, A., Beugnon, G., and Cheng, K.** (2011a). Landmarks or panoramas: what do
740 navigating ants attend to for guidance? *Front. Zool.* **8**, 21

- 741 **Wystrach, A., Beugnon, G., and Cheng, K.** (2012). Ants might use different view-matching
742 strategies on and off the route. *J. Exp. Biol.* **215**, 44-55.
- 743 **Wystrach, A., Mangan, M., Philippides, A., & Graham, P.** (2013). Snapshots in ants? New
744 interpretations of paradigmatic experiments. *J. Exp. Biol.* **216**, 1766-1770.
- 745 **Wystrach, A., Schwarz, S., Baniël, A., and Cheng, K.** (2013). Backtracking behaviour in lost
746 ants: an additional strategy in their navigational toolkit. *Proc. Roy. Soc. B* **280**, 20131677.
- 747 **Wystrach, A., Lagogiannis, K., & Webb, B.** (2016). Continuous lateral oscillations as a core
748 mechanism for taxis in *Drosophila* larvae. *Elife*, 5, e15504.
- 749 **Wystrach, A., Schwarz, S., Graham, P., and Cheng, K.** (2019). Running paths to nowhere:
750 repetition of routes shows how navigating ants modulate online the weights accorded to
751 cues. *Animal Cognition* **22**, 213-222.
- 752 **Wystrach, A., Schwarz, S., Schultheiss, P., Beugnon, G., & Cheng, K.** (2011b). Views,
753 landmarks, and routes: how do desert ants negotiate an obstacle course? *J. Comp.*
754 *Physiol. A* **197**, 167-179.
- 755 **Wystrach, A., Schwarz, S., Schultheiss, P., Beugnon, G., & Cheng, K.** (2011c). Views,
756 landmarks, and routes: how do desert ants negotiate an obstacle course? *J. Comp.*
757 *Physiol. A* **197**, 167-179.
- 758 **Wystrach, Antoine, et al.** (2019)"Avoiding pitfalls: Trace conditioning and rapid aversive
759 learning during route navigation in desert ants." *bioRxiv*: 771204.**Zahedi, M.S., and Zeil,**
760 **J.** (2018). Fractal dimension and the navigational information provided by natural scenes.
761 *PLoS ONE* **13**, e0196227.
- 762 **Zeil, J., and Fleischmann, P.** (2019). The learning walks of ants. *Myrmecol. News* (under
763 review).
- 764 **Zeil, J., Hofmann, M.I., and Chahl, J.S.** (2003). Catchment areas of panoramic snapshots in
765 outdoor scenes. *J. Opt. Soc. Am. A* **20**, 450-469.
- 766 **Zeil, J., Narendra, A., and Stürzl, W.** (2014). Looking and Homing: How displaced ants decide
767 where to go. *Phil. Trans. Roy. Soc. B* **369**, 20130034.
- 768 **Zeil, J.** (2012). Visual homing: an insect perspective. *Curr. Opin. Neurobiol.* **22**, 85-93.
- 769

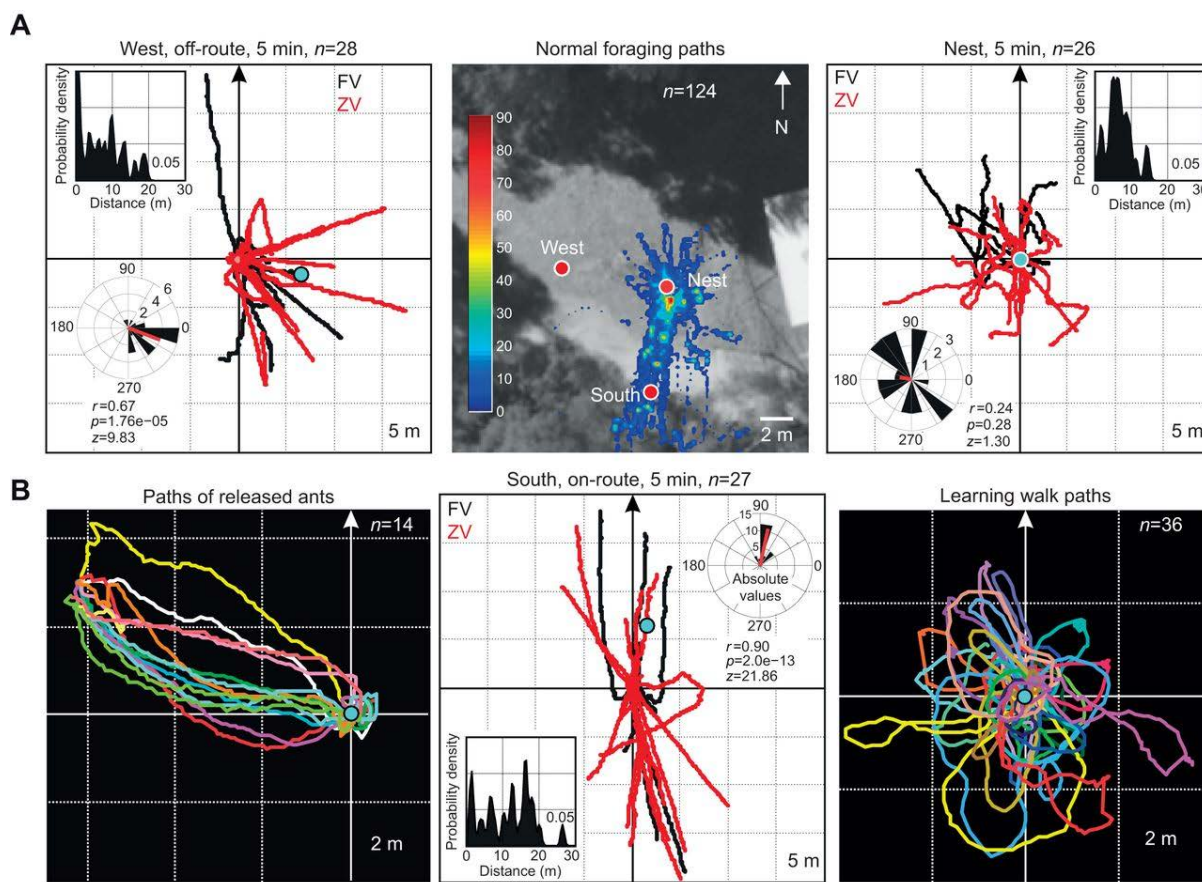
770 Figures and Legends

771 **Figure 1**



773 **Figure 1** **Experimental set-up and agent-based modelling.** (A) Three views of the air-
774 cushioned trackball contraption and the tethered ant. (B) Schematic map of the attractive
775 (attractive) and repellent (repellent) memorized views along the foraging route and around
776 the nest that constituted the attractive and repellent memory bank. (C) Schematic
777 distribution of familiarity (1) and un-familiarity values (-1) for attractive and repellent views
778 at the four release locations and the result of their integration. Note that distributions at the
779 nest and at the completely unfamiliar site are uniform for different reasons: high familiarities
780 for both attractive and repellent views at the nest and low familiarities for both view sets at
781 the completely unfamiliar site. (D) A 'neuro-schematic' summary of the model comparing a
782 current view with a repellent and a attractive view memory bank and the integration of the
783 output providing a steering command. (E) The paths generated by the simulation reproduce
784 the details of real ant paths better when the regular alternation of path direction is
785 implemented at every 4th step, rather than at each successive step (as has been done in the
786 present study).

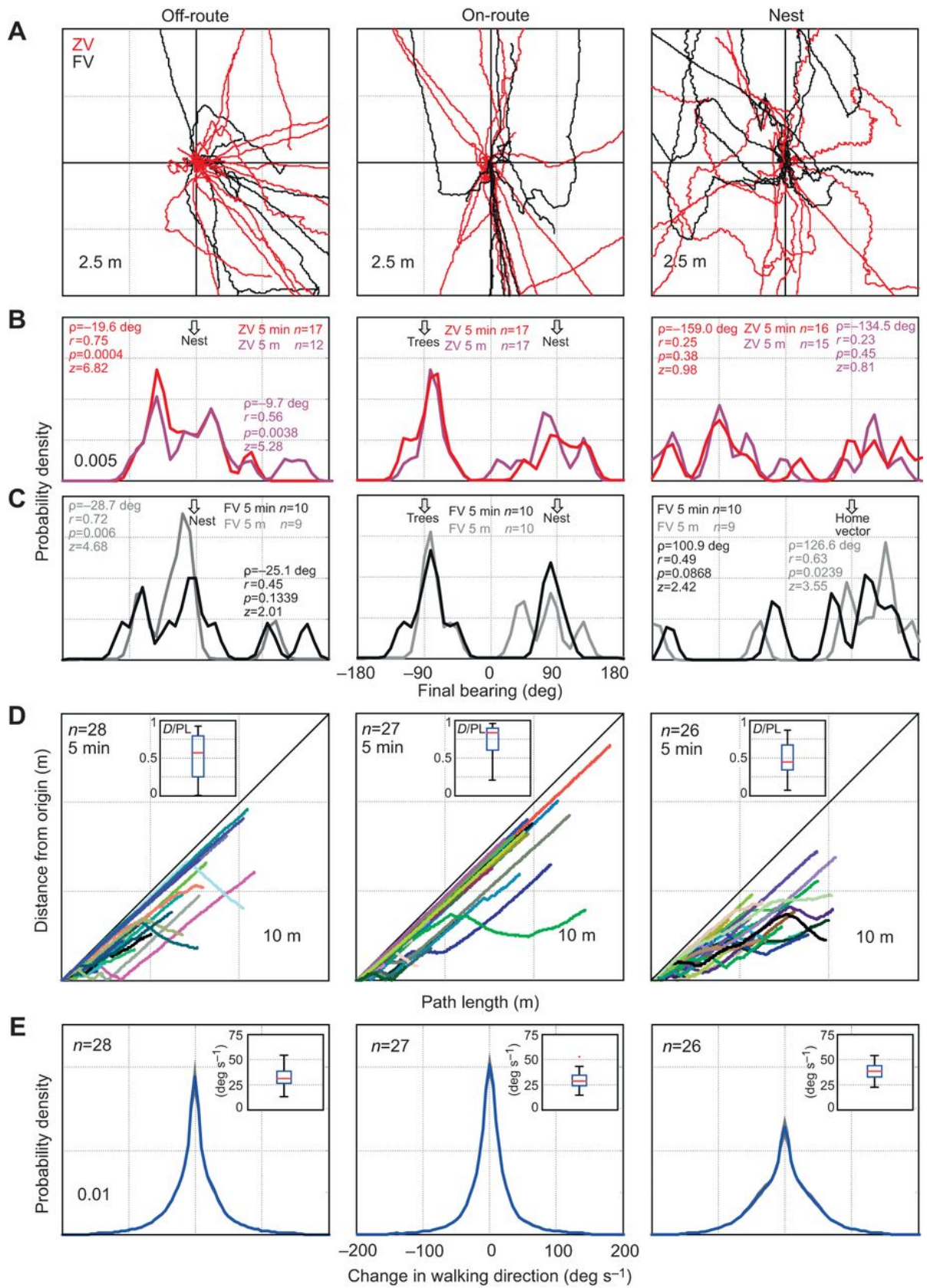
787

788 **Figure 2**

789

790 **Figure 2** **The behaviour of tethered ants at three locations in their natural foraging**
 791 **environment.** Top centre panel: Aerial photograph of the nest area with Off-route, Nest and
 792 On-route locations marked by red circles. False colour-coded area shows the 2D probability
 793 density of 124 outward going paths of foraging ants that operated from this nest and were
 794 tracked with Differential GPS over a period of two years. See colour bar for scale and Fig. S1
 795 for individual paths. Intended paths of tethered ants are shown for the Off-route location (top
 796 left panel), the Nest location (top right panel) and the On-route location (bottom centre
 797 panel), with the paths of zero-vector (ZV) ants shown in red and those of full-vector (FV)
 798 in black. The nest location is indicated by a blue circle. Insets show for both FV and ZV ants
 799 the probability density of virtual distances from the starting point reached after 5 minutes
 800 and circular histograms of final bearings with red line indicating the length and direction of
 801 the mean vector; r : resulting vector length; p : probability of rejecting hypothesis of uniform
 802 distribution and z : z-statistic of Rayleigh test of uniformity. Bottom left panel: Paths of 14 ants
 803 released just north of the Off-route location and tracked with Differential GPS. Bottom right
 804 panel: Learning walk paths of ants around the nest, recorded with Differential GPS.

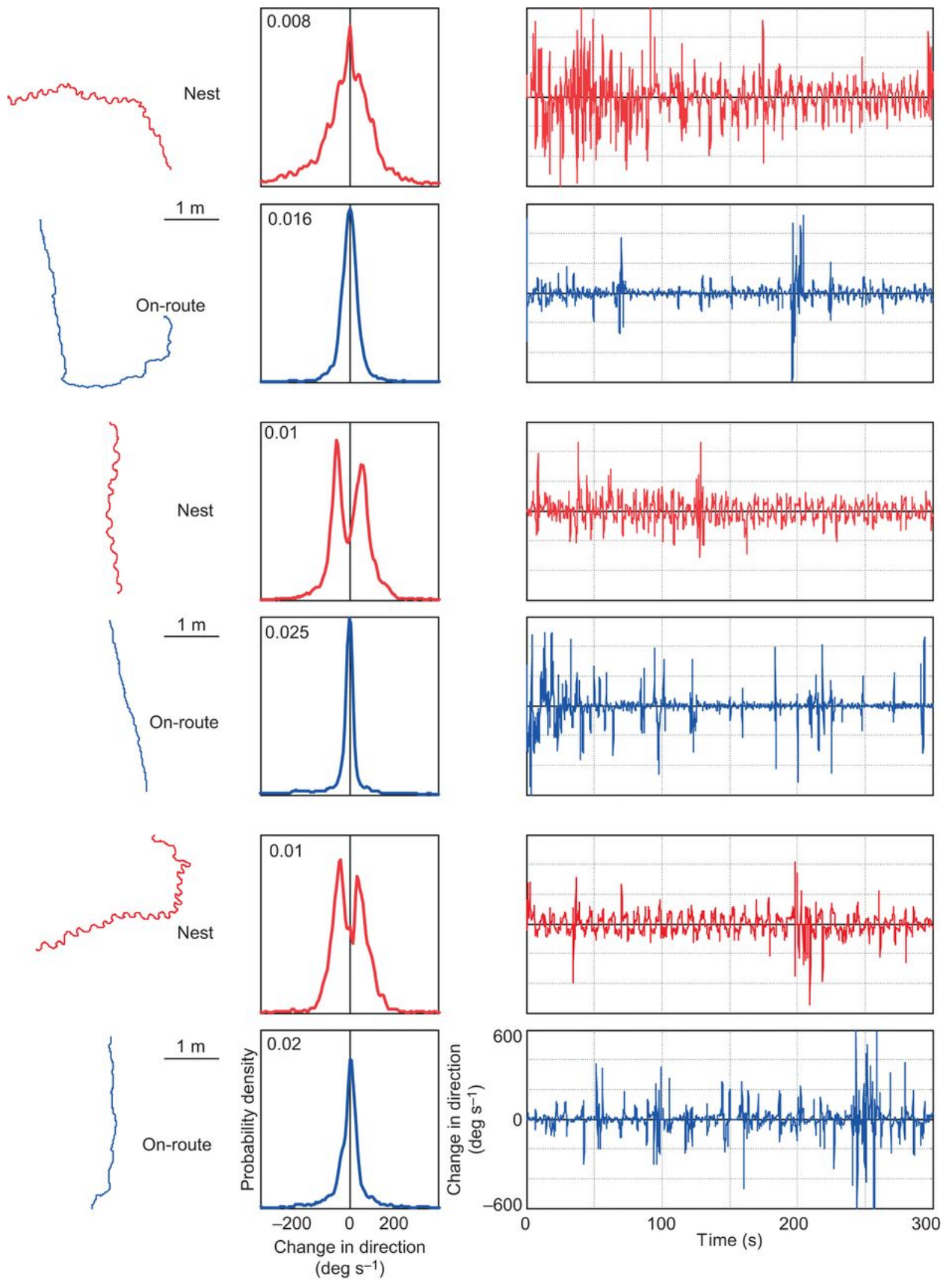
805 **Figure 3**



807 **Figure 3** **Quantitative analysis of behavioural differences at the Off-route, On-route**
808 **and Nest location.** (A) Initial intended paths of tethered ants at a finer scale. The paths of ZV
809 ants are shown in red and those of FV ants in black. (B) Distributions of final bearings of ZV
810 ants after 5 minutes (red) or when having reached a virtual distance of 5 m from the start
811 (purple) at the three locations. Probability densities determined with 9° bandwidth of the
812 kernel smoothing window; North at $+90^\circ$. Inset numbers show results of circular statistics
813 (Rayleigh test of uniformity) with ρ : mean vector direction; r : mean vector length; p :
814 probability of uniformity; z : z-statistic. Arrows mark the direction of nest and trees. (C)
815 Distributions of final bearings for FV ants after 5 minutes (black) or when having reached a
816 virtual distance of 5 m from the start (grey). Arrows mark the direction of nest, trees and
817 home vector. Otherwise conventions as in (B). (D) Distance from start over path length for
818 the first 5 minutes of paths at the three locations. Paths are randomly coloured. Insets show
819 boxplots with median marked red for the ratios of distance over path length at the end of 5
820 minutes. See Fig. S2B for statistics. (E) Distributions of changes in walking direction for all 5
821 min paths at the three locations. Shown are the means of individual distributions (blue) and
822 standard errors in grey (not visible). Insets show boxplots for the distributions of individual
823 means. See Fig. S2C and D for statistics.

824

825 **Figure 4**



827 **Figure 4** **Ants walk differently at the Nest (red) and the On-route (blue) location.**

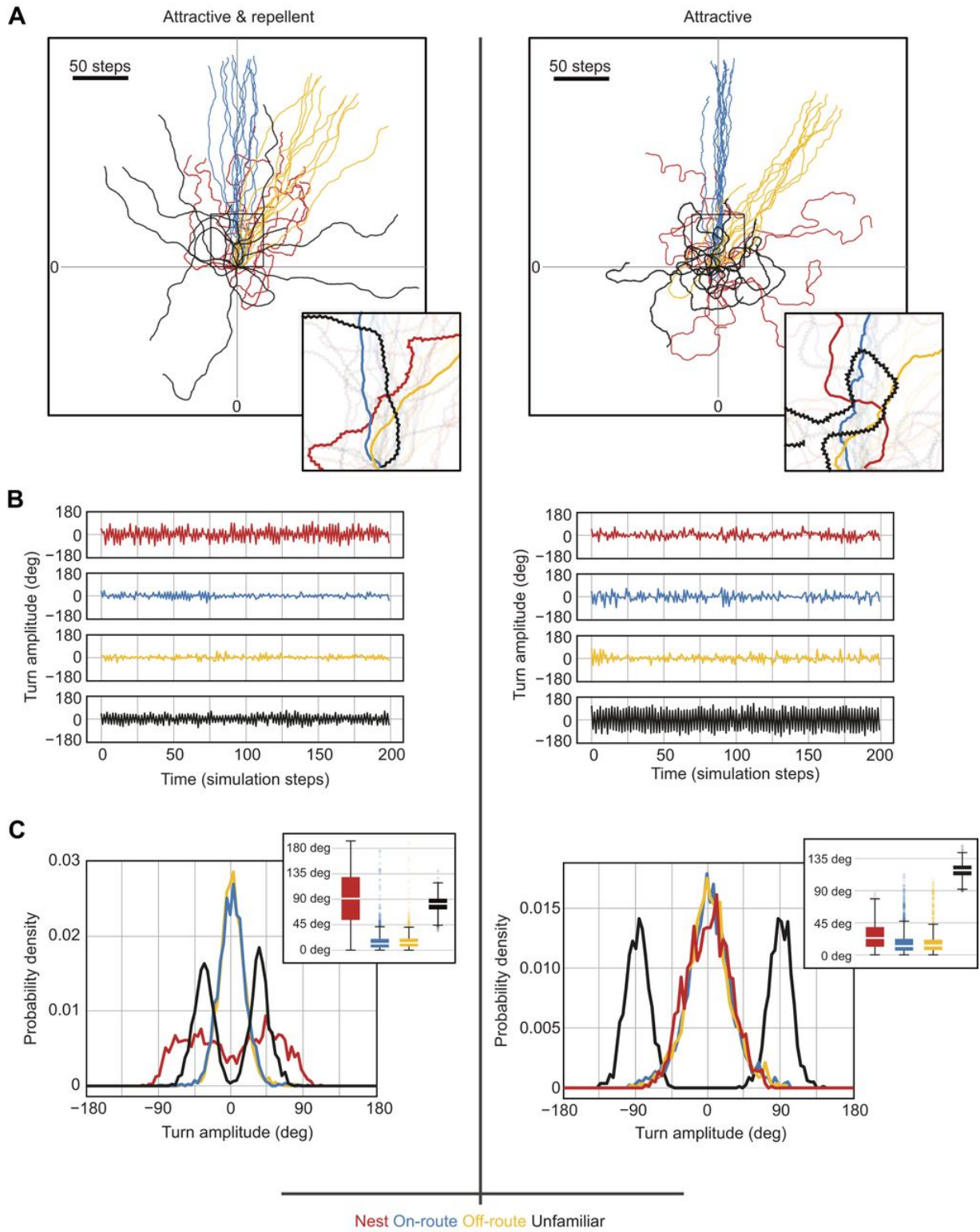
828 Shown are path segments on the left, the distributions of changes in walking direction during
829 the first 5 minutes in the middle row and the time series of changes in walking direction over
830 5 minutes on the right for three ants (top, centre, bottom), each recorded at the nest and at
831 the on-route location. Changes in walking direction were determined at 11fps to reduce
832 measurement noise. See Fig. S3 for auto-correlation functions.

833

834

835 **Figure 5**

836



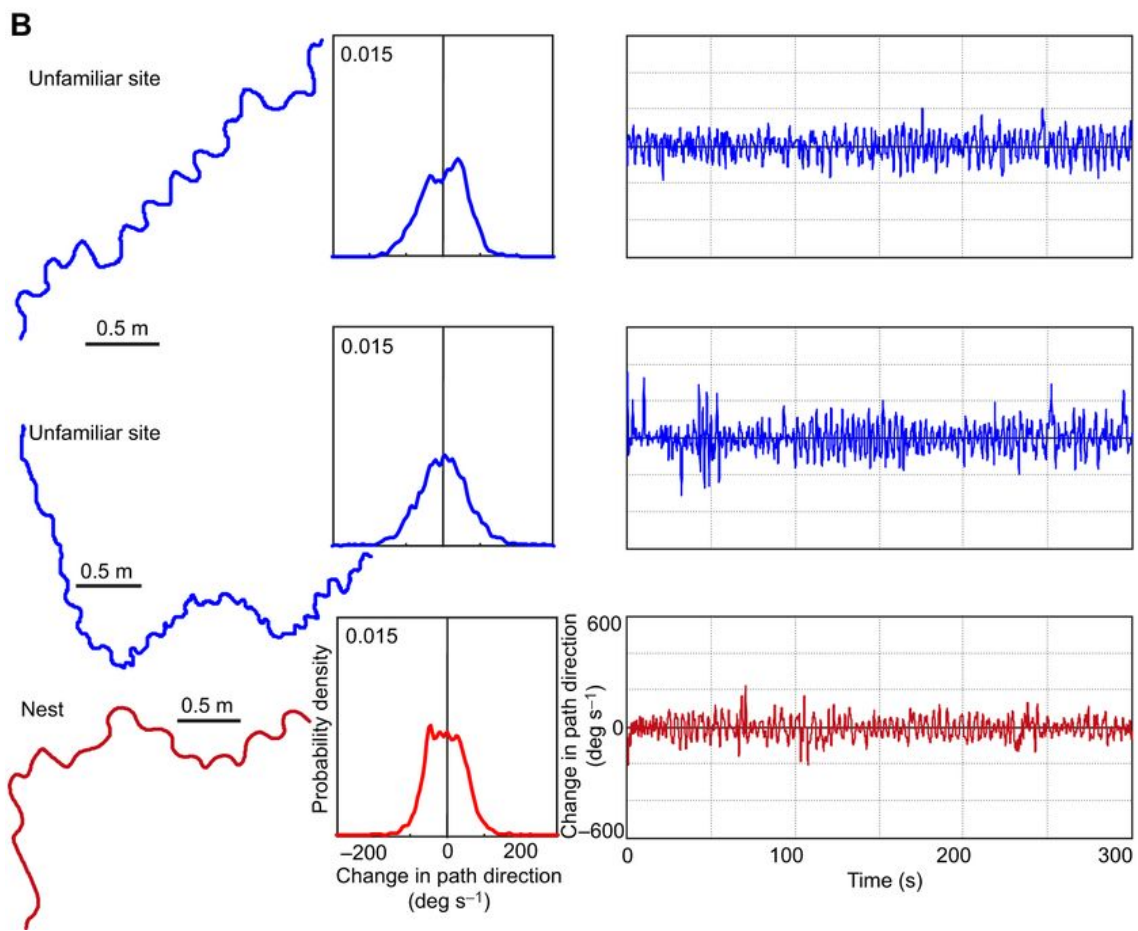
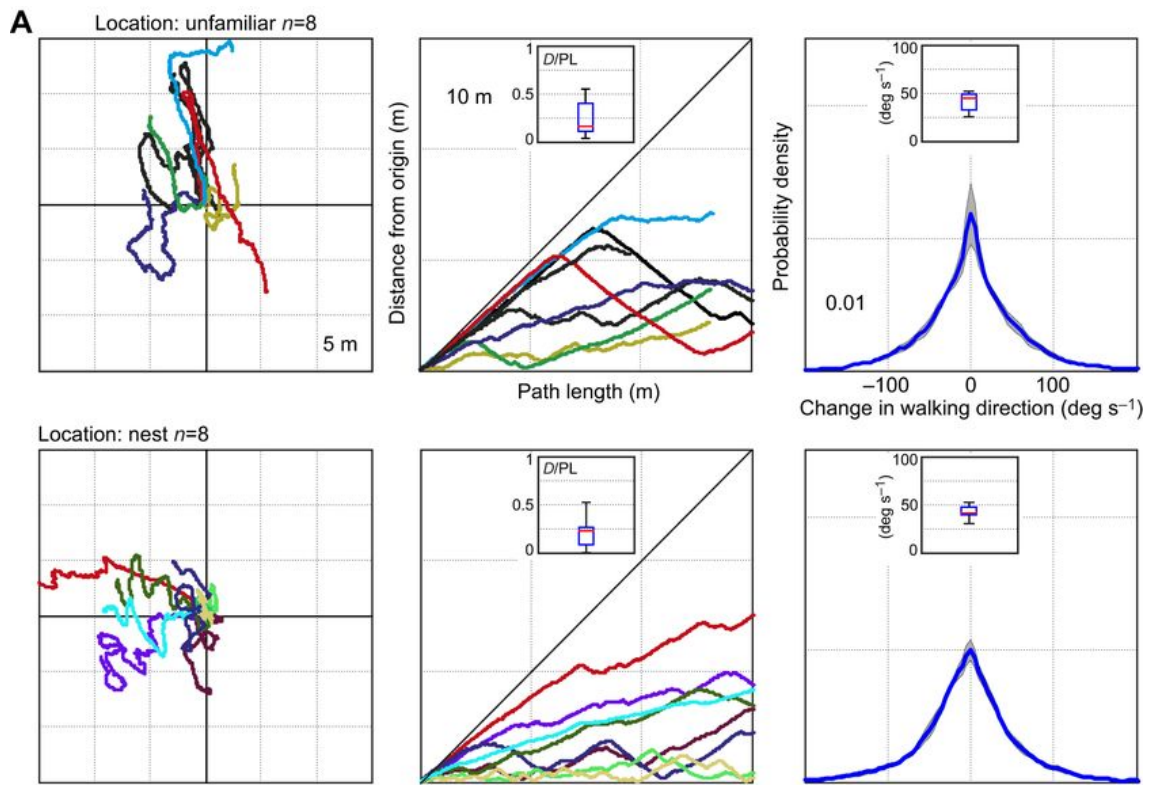
837

838

839 **Figure 5** **The results of agent-based visual navigation using both attractive and**
840 **repellent views (left column) and attractive views only (right column).** We simulated ten
841 agents walking 200 steps at each nest (red), on-route (blue), off-route (yellow) and unfamiliar
842 (black) release locations. (A) Resulting paths. Insets show close-up details of example paths.
843 (B) Turn amplitudes over time (simulation steps) for one example at each of the release
844 locations. (C) Probability densities of turn amplitudes at the four release locations. Inset show
845 box and whisker plots for the same distributions.

846

847 **Figure 6**



849 **Figure 6** **Ants behave in a similar way at a completely unfamiliar location and at the**
850 **nest.** (A) Top row: Paths (left), distance from start over path length (middle) and probability
851 density of changes in walking direction (right) for 8 tethered ants at a completely unfamiliar
852 location. Bottom row: Same for 8 ants at the nest location. Insets in middle panels show
853 boxplots of final distance to path length ratios after 5 minutes, which are not different
854 between the unfamiliar and the nest location (Wilcoxon Rank Sum test unfamiliar vs nest
855 location: $p=0.7984$, ranksum=71). Insets in right panels show the boxplots of mean absolute
856 values of changes in path direction over 5 minutes, which are not different between the
857 unfamiliar and the nest location (Wilcoxon Rank Sum test unfamiliar vs nest location:
858 $p=0.9591$, ranksum=67). (B) Example paths (left), probability density of changes in path
859 direction (middle) and time series of changes in path direction (right) for two ants at the
860 unfamiliar site (blue) and one ant over the nest (red).

861

862

863

864

865

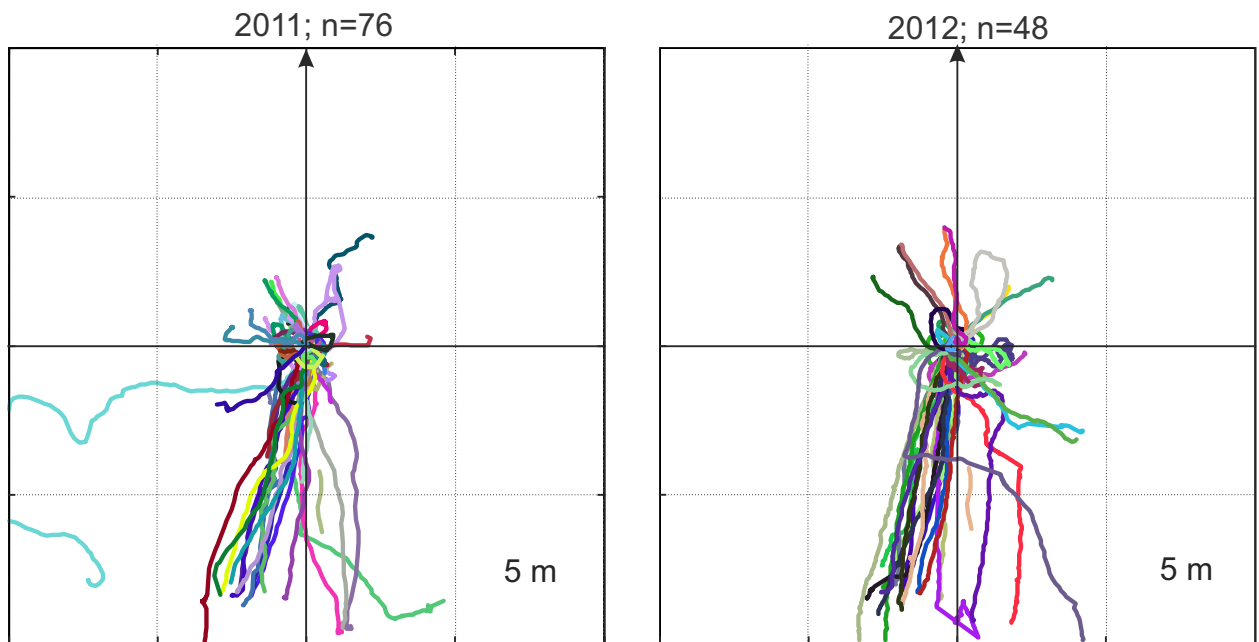


Figure S1 Foraging patterns at the *M. croslandi* nest used in this study. Panels show the individual paths of foragers as they have been recorded with differential GPS over a period of two years. These paths provided the original data for the 2D histogram shown in the middle panel of Fig. 1B.

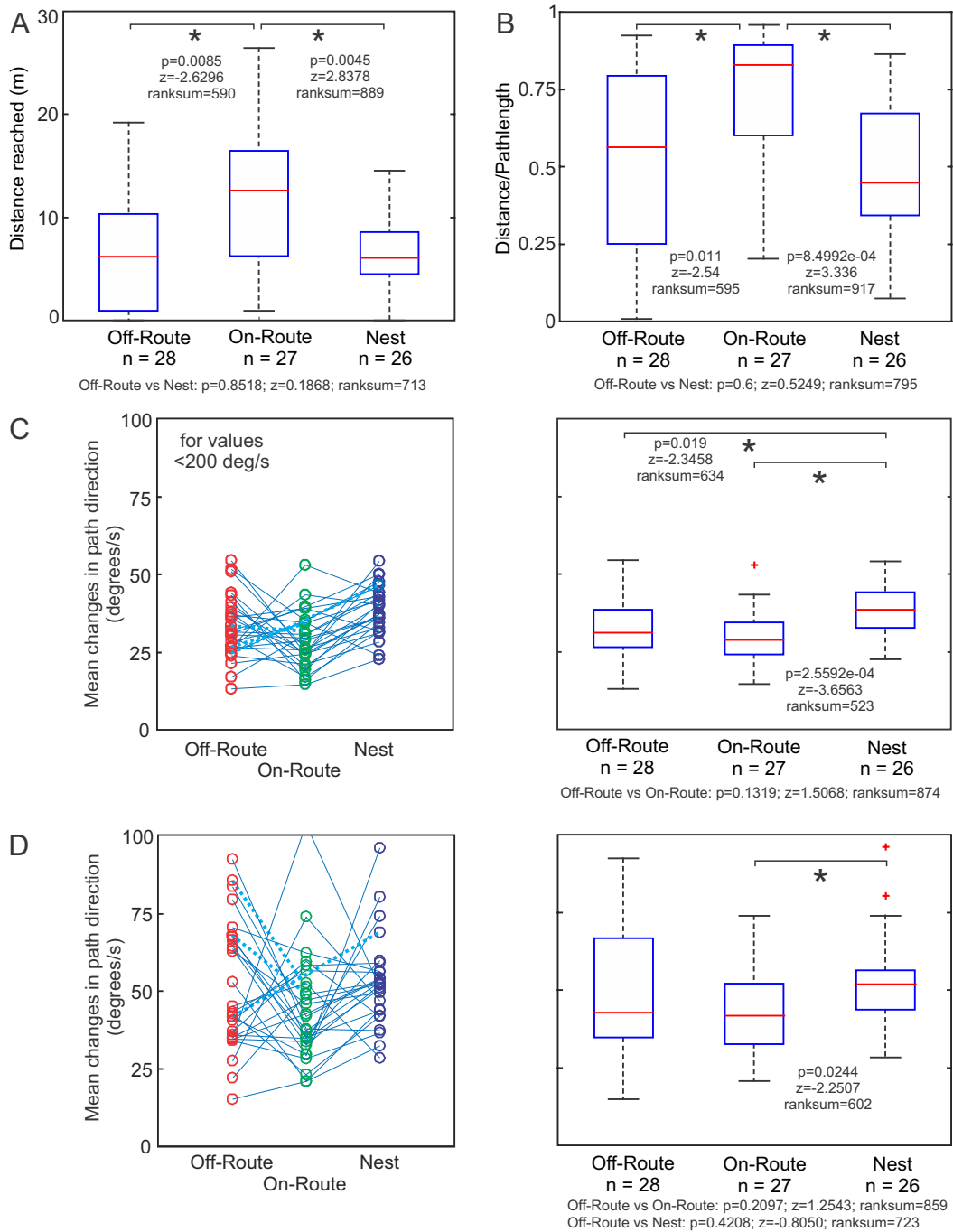


Figure S2 Quantitative analysis of behavioural differences between Off-route, On-route and Nest locations. (A) Box plots of distances reached after 5 minutes at the three locations. Significant comparisons with a Wilcoxon Rank sum test are marked by a star and values are shown inside the panel. Values for on-significant comparisons are shown below the panel. (B) Box plots of distance over path length ratios after 5 minutes at the three locations. Otherwise conventions as in (A). (C) Left panel: Individual means of the changes in path direction (absolute values < 200°/s, determined at 11fps) for the first 5 minutes with means of individual ants connected by blue lines. Dashed lines mark cases where an ant was released at two locations only. Right panel: Boxplots of mean changes in path direction with significant differences as determined by Wilcoxon Rank Sum test marked by a star and values shown as inset. Values for non-significant comparisons are shown below the panel. (D) Same for the means and distributions of all absolute values of changes in path direction. Otherwise conventions as before.

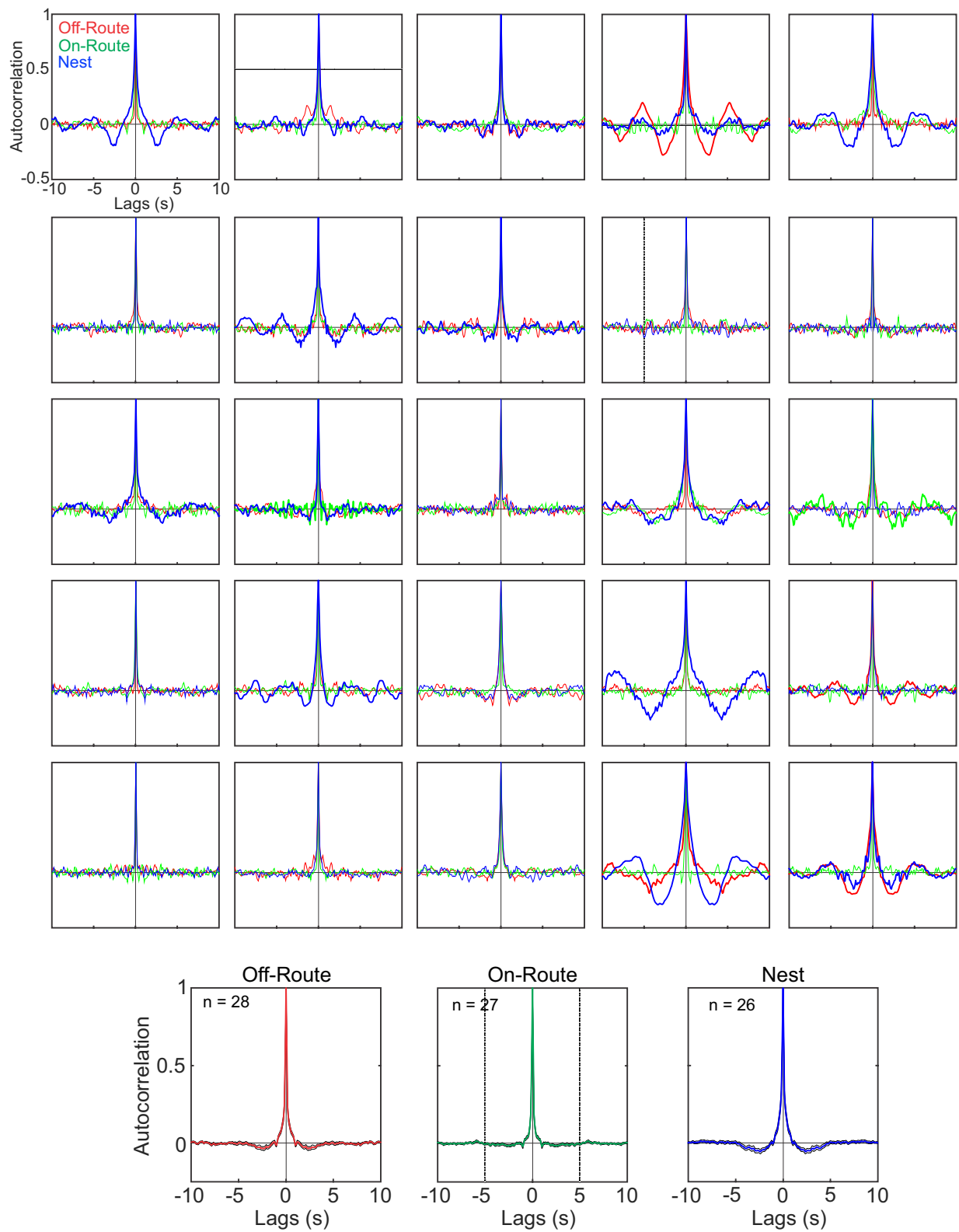


Figure S3 Comparison of auto-correlation functions of 5 minute time series of changes in path direction at the three locations. Off-route: red; On-route: green; Nest: blue for each of 25 ants that were tested at all three locations. Bottom panels show mean auto-correlations for all ants at the three locations.